Available online at www.sciencedirect.com
ScienceDirect
Procedia Computer Science 1 (2012) 735–744
Procedia Computer Science
www.elsevier.com/locate/procedia

International Conference on Computational Science, ICCS 2010

Computing of Gas Flows in Micro- and Nanoscale Channels on the Base of the Boltzmann Kinetic Equation

Yu.A. Anikin[a,b], E.P. Derbakova[a,b], O.I. Dodulad[a,b], Yu.Yu. Kloss[a,b], D.V. Martynov[a,b], O.A. Rogozin[a,b], P.V. Shuvalov[a,b], F.G. Tcheremissine[a,c,*]

[a] *Moscow Institute of Physics and Technology*
[b] *Russian Research Center "Kurchatov Institute"*
[c] *Dorodnicyn Computing Centre of RAS*

Abstract

The paper describes the methodology of computing gas flows in narrow micro- and nanoscale channels on the basis of finite-difference solution of the Boltzmann kinetic equation using the conservative projection method of collision integral calculation. Mathematical framework of the method is considered and the problem solving environment for calculation of the above mentioned flows is described. Examples of the flow calculations in the plane and 3D geometry are given.

Keywords: computing of gas flows, micro- and nanochannels, Boltzmann equation, problem solving environment, Knudsen pump
PACS: 47.61.-kf, 47.11.-j, 47.45.-n, 47.45.Gx, 47.40.Nm

1. Introduction

Investigation of gas flows in micro- and nanochannels is now of practical interest due to development of miniature devices of various purposes using gas transfer between vessels, transfer of heat by gas, or a change in the gas mixture composition [1, 2]. These devices are characterized by two geometrical scales, one of which is defined by the channel length and sizes of vessels connected by the channel and the other by the channel diameter, with the second scale being much less than the first one and commensurate with the gas molecule free path. The commensurability of the lesser flow scale with molecule free path calls for application of kinetic theory methods. Due to the large difference in the scales the flow velocity is usually much less than the sound velocity, while gas parameters slowly change along the flow. A so-called slow flow pattern is implemented, where the molecular velocity distribution function is little different from the Maxwellian distribution function almost everywhere. This flow pattern allows optimizing computational methods as described below.

*Corresponding author
Email addresses: kloss@mnpt.kiae.ru (Yu.Yu. Kloss), shuvalov.pavel@gmail.com (P.V. Shuvalov), tcherem@ccas.ru (F.G. Tcheremissine)

1877-0509
doi:10.1016/j.procs.2010.04.079

A reliable basis for studying flows within the framework of the kinetic theory is the Boltzmann kinetic equation, however, the complexity of its numerical solution has motivated the search for alternative, less time-consuming, though not rigorously mathematically justified approaches. One of such approaches is the Direct Simulation Monte Carlo method (DSMC method) [3] where solution of the kinetic equation is replaced with computer simulation of movements and collisions of a large number of points representing gas molecules. This method was successfully used in supersonic aerodynamics, however, its application for analysis of slightly disturbed flows proved to be extremely inefficient due to non-removable noise [4]. The other commonly used approach is the use of "model" kinetic equations where the complex Boltzmann collision integral is replaced with a simple relaxation form. Quite a lot of interesting results have been obtained along this line, but their reliability is not guaranteed since the model equations themselves are not justified. From physical standpoint, a serious drawback of the model equations is the velocity-independent relaxation time, while in real gas the molecular collision frequency changes several times over a substantial molecular velocity range [5].

For the long time, the major challenge in numerical solution of the Boltzmann equation, besides its high dimensionality, had been associated with the lack of a conservative method of the collision integral calculation. This problem has been solved in [6] and then the conservative method of calculating the collision integral has been essentially improved in [7, 8]. In the work presented herein all calculations were performed using this method and its generalization for a gas mixture.

2. Mathematical and theoretical framework

2.1. Monocomponent gas

The gas density $n(\mathbf{x},t)$, temperature $T(\mathbf{x},t)$, velocity $\mathbf{U}(\mathbf{x},t)$ and other parameters are calculated by numerical integration on velocity $\boldsymbol{\xi}$ of distribution function $f(\boldsymbol{\xi},\mathbf{x},t)$ determined from solution of the Boltzmann equation:

$$\partial f/\partial t + \boldsymbol{\xi}\cdot\partial f/\partial \mathbf{x} = I(f,f) \tag{1}$$

Equation (1) is solved by the finite-difference method on fixed grid in velocity and coordinate space. The computational domain in the coordinate space is broken down into cells, in the general case having an arbitrary shape and a finite volume method is used for approximation of the equation left-hand side. A spherical domain Ω on a uniform grid with a spacing $h_v = 2V_{max}/N_0$, where N_0 is the number of nodes for each velocity coordinate, is chosen as the velocity space. The sphere centre may be displaced relative to zero depending on the problem. The maximum velocity V_{max} is taken equal to $4.8\sqrt{kT_{max}/m}$, where T_{max} is the maximum temperature.

Equation (1) splits into two parts: the transport equation representing the left side and the relaxation problem. The splitting takes the form $S_\tau = A_{\tau/2}C_\tau A_{\tau/2}$, where S_τ is the operator transforming the solution at t_0 to the solution at $t_0+\tau$, A_τ is the the operator of solving the transport equation $\partial f/\partial t+\boldsymbol{\xi}\cdot\partial f/\partial\mathbf{x}=0$ beginning at steps τ and C_τ is the operator of solving the relaxation problem $\partial f/\partial t = I(f,f)$.

For monatomic gas, the collision integral takes the form [5]:

$$I(f,f) = \int_{-\infty}^{\infty}\int_0^{2\pi}\int_0^{b_m}(f'f'_* - ff_*)gbdbd\varphi d\boldsymbol{\xi}_* \tag{2}$$

By introducing the following notation: $\phi(\boldsymbol{\xi}_\gamma) = \delta(\boldsymbol{\xi}-\boldsymbol{\xi}_\gamma)+\delta(\boldsymbol{\xi}_*-\boldsymbol{\xi}_\gamma)-\delta(\boldsymbol{\xi}'-\boldsymbol{\xi}_\gamma)-\delta(\boldsymbol{\xi}'_*-\boldsymbol{\xi}_\gamma)$, where δ is the Dirac delta function and $\boldsymbol{\xi}'$ and $\boldsymbol{\xi}'_*$ are post collision velocities that are arguments of functions f' and f'_*, we present the collision integral in point $\boldsymbol{\xi}_\gamma$ as follows:

$$I(\boldsymbol{\xi}_\gamma) = \frac{1}{4}\int_{-\infty}^{\infty}\int_{-\infty}^{\infty}\int_0^{2\pi}\int_0^{b_m}\phi(\boldsymbol{\xi}_\gamma)(f'f'_* - ff_*)gbdbd\varphi d\boldsymbol{\xi}d\boldsymbol{\xi}_* \tag{3}$$

In equation (3), integration is performed numerically on the grid $\boldsymbol{\xi}_{\alpha_\nu}, \boldsymbol{\xi}_{\beta_\nu}, b_\nu, \varphi_\nu$ consisting of N_ν nodes in the 8-dimensional domain $\Omega \times \Omega \times [0, 2\pi] \times [0, b_{max}]$. Pre-collision velocities $\boldsymbol{\xi}_{\alpha_\nu}$, $\boldsymbol{\xi}_{\beta_\nu}$ are selected in the velocity grid nodes. Post-collision velocities $\boldsymbol{\xi}'_{\alpha_\nu}$ and $\boldsymbol{\xi}'_{\beta_\nu}$ do not get in the nodes in the general case. For each velocity $\boldsymbol{\xi}'_{\alpha_\nu}$ there is determined a pair of nodes $\boldsymbol{\xi}_{\lambda_\nu}$ and $\boldsymbol{\xi}_{\mu_\nu}$ that approximates the velocity on the velocity grid and for velocity $\boldsymbol{\xi}'_{\beta_\nu}$ there are chosen nodes $\boldsymbol{\xi}_{\lambda_\nu+s_\nu}$ and $\boldsymbol{\xi}_{\mu_\nu-s_\nu}$ that are symmetric about the total velocity $\mathbf{g}_\nu = \boldsymbol{\xi}_{\alpha_\nu} + \boldsymbol{\xi}_{\beta_\nu}$, after which the delta function in formula (3) is represented in the following form: $\delta(\boldsymbol{\xi}'_{\alpha_\nu} - \boldsymbol{\xi}_\gamma) = (1-r_\nu)\delta(\boldsymbol{\xi}_{\lambda_\nu} - \boldsymbol{\xi}_\gamma) + r_\nu\delta(\boldsymbol{\xi}_{\mu_\nu} - \boldsymbol{\xi}_\gamma)$, where factor r_ν is found from the energy conservation law: $(\boldsymbol{\xi}'_{\alpha_\nu})^2 + (\boldsymbol{\xi}'_{\beta_\nu})^2 = (1-r_\nu)(\boldsymbol{\xi}^2_{\lambda_\nu} + \boldsymbol{\xi}^2_{\mu_\nu}) + r_\nu(\boldsymbol{\xi}^2_{\lambda_\nu+s_\nu} + \boldsymbol{\xi}^2_{\mu_\nu-s_\nu})$. The following power interpolation is used for approximation of the product of distribution functions after the collision:

$$f'_{\alpha_\nu} f'_{\beta_\nu} = (f_{\lambda_\nu} f_{\mu_\nu})^{1-r_\nu} (f_{\lambda_\nu+s_\nu} f_{\mu_\nu-s_\nu})^{r_\nu} \tag{4}$$

This interpolation provides strict equality of the collision integral of the Maxwellian distribution function to zero, which is especially important for simulation of slow flows and flows containing slightly disturbed regions.

Let the solution take the form $f = f_M + \varepsilon f^{(1)}$ where $\varepsilon f^{(1)}$ is the deviation from the Maxwell distribution and $\varepsilon \ll 1$. Substituting this solution in the collision integral and considering (4), we arrive at:

$$I(f, f) = I(f_M, f_M) + 2\varepsilon I(f_M, f^{(1)}) + \varepsilon^2 I(f^{(1)}, f^{(1)}) \tag{5}$$

Since the principal part of integral $I(f_M, f_M)$ is calculated exactly, it follows from (5) that the collision integral calculation error reduces approximately $(2\varepsilon)^{-1}$ times.

Thus in the projection method only one 8-fold integral (3) is calculated instead of calculating N_0 5-fold integrals (2), which is more economical. Irrespective of the number of integrating grid nodes, strict observance of the collision integral conservation laws and its equality to zero on the Maxwellian distribution function are ensured.

The calculation of collision integral (3) consists of a preparation step that is performed only once and calculation of collision integrals in each space node and at each time step. At the preparation step, a set of a large number of 8-dimensional integrating grids $\boldsymbol{\xi}_{\alpha_\nu}, \boldsymbol{\xi}_{\beta_\nu}, b_\nu, \varphi_\nu$ is generated on the basis of Korobov grids [9]. Korobov grids ensure higher accuracy of multidimensional integral evaluation compared to random node grids. Post-collision velocities $\boldsymbol{\xi}'_{\alpha_\nu}$ and $\boldsymbol{\xi}'_{\beta_\nu}$, relative velocities g_ν and factors r_ν are calculated for each integrating grid $\boldsymbol{\xi}_{\alpha_\nu}, \boldsymbol{\xi}_{\beta_\nu}, b_\nu, \varphi_\nu$ at a specified molecular potential. During the calculation, one of such extended grids is selected in a random manner at each time step and used for calculation of integral (3) in all nodes of the physical space.

2.2. Gas mixture

Generalization of the conservative projection method of calculating the collision integral for the case of gas mixture is implemented by going from the velocity space $\boldsymbol{\xi}_i$ to the molecule momentum space $\mathbf{p}_i = m_i\boldsymbol{\xi}_i$, where m_i is the molecular mass of the i-th mixture component [10, 11]. The system of kinetic equations for the N-component gas mixture will take the form:

$$\frac{\partial f_i}{\partial t} + \frac{\mathbf{p}_i}{m_i} \cdot \frac{\partial f_i}{\partial \mathbf{x}} = \sum_{j=1}^{N} \int (f'_i f'_j - f_i f_j) g_{ij} b db d\varphi d\mathbf{p}_j \tag{6}$$

The collision integral for the i-th equation is defined by the following formula:

$$I_i(\mathbf{p}_\gamma) = \frac{1}{4} \sum_k \sum_j \int_{-\infty}^{\infty} \int_{-\infty}^{\infty} \int_0^{2\pi} \int_0^{b_m} \phi_i(\mathbf{p}_\gamma)(f'_k f'_j - f_k f_j) g b db d\varphi d\mathbf{p}_k d\mathbf{p}_j \tag{7}$$

Operator $\phi_i(\mathbf{p}_\gamma)$ in (7) is similar to the projection operator for a monocomponent gas. The other calculations are performed similarly to the monocomponent gas case.

2.3. Consideration of rotational degrees of freedom

Consideration of the effect of rotational degrees of freedom may be required for molecular gases since the characteristic time of rotational relaxation is comparable with the time between molecular collisions. To this end the generalized Boltzmann equation (Wang Chang-Uhlenbeck equation) can be used [12]. The method of solving this equation is proposed in [13], however this calls for significant computational resources and we use an approximate approach based on application of the 2LRT model of rotation-translation transitions [14].

2.4. Organization of calculations

We have developed a problem-solving environment [15] that allows simulating flows in channels of different geometry at specified physical properties of the gas and gas/surface interaction model. It includes algorithms of building grids in the coordinate space and in the velocity (momentum) space, algorithms of finite-difference approximation of the advection operator of the kinetic equation of the first and second order of accuracy, parallel computing algorithms built around the domain decomposition technique, data input/output interface and graphics programs.

The number of computational nodes varied from 10^7 to 10^9, and the size of the Korobov grids laid in the interval from $5 \cdot 10^4$ up to 10^6 points depending on the problem. The paralleling algorithm provides the linear growth of the performance with increasing number of computational nodes [15, 16]. The largest computational time was for the problem from chapter 3.4, it took 24 hours using 20 dual-core Xeon 5160 3HGz (the simulation was performed with the MIPT-60 supercomputer).

3. Examples of simulation

Presented below are fragments of numerical investigations of various flows performed using the methodology described above.

3.1. Flow structure of thermal creep

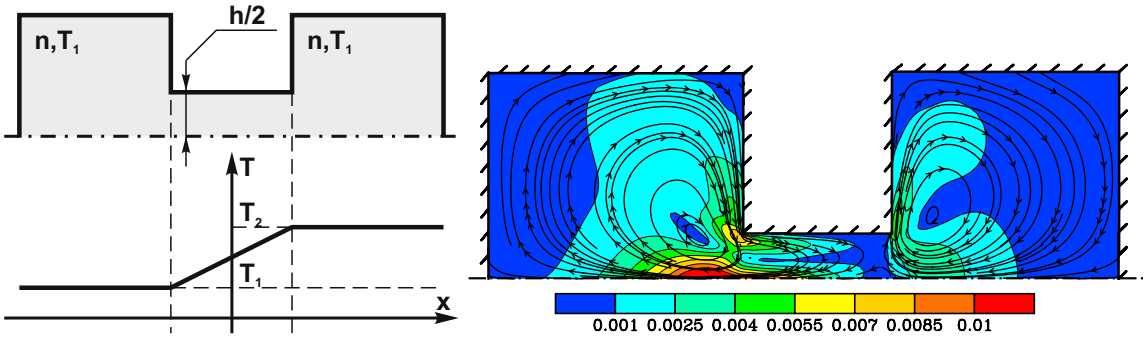

Figure 1: (a) Thermal creep problem geometry (b) Streamlines in steady state, Kn = 0.1

Thermal creep flow develops along a nonuniformly heated surface and is a driving force of thermomolecular Knudsen pumps operating in the rarefied gas regime. The simplest Knudsen pump is shown in Figure 1(a). It represents two vessels connected by a narrow channel where a temperature gradient is established. The flow is considered in plane geometry. Let the wall temperature of the left-hand vessel be T_1 and the wall temperature of the right-hand vessel be $T_2 = 2T_1$. A gas flow to the hot vessel will develop near the channel walls due to thermal creep, which will cause a reverse flow along the channel center. In steady-state conditions, these flows equilibrate, which produces vortex flows in the channel and vessels. The flow was calculated on a rectangular grid with a variable spacing in the physical space. The left-hand side of the Boltzmann equation was approximated by the explicit TVD scheme of the second order of accuracy.

The flow structure is shown in Figure 1(b) in the form of streamlines taking into account the flow symmetry. The Knudsen number $\mathrm{Kn} = \lambda/h$ is defined from the molecular mean free path λ in the left-hand vessel and from the channel width h. The free path at $T_1 = 300K$ and atmospheric pressure is $\lambda \approx 0.1\ \mu m$, which gives $h \approx 1\ \mu m$ and the maximum dimensional velocity value $v_{max} = 3.5\ m/s$.

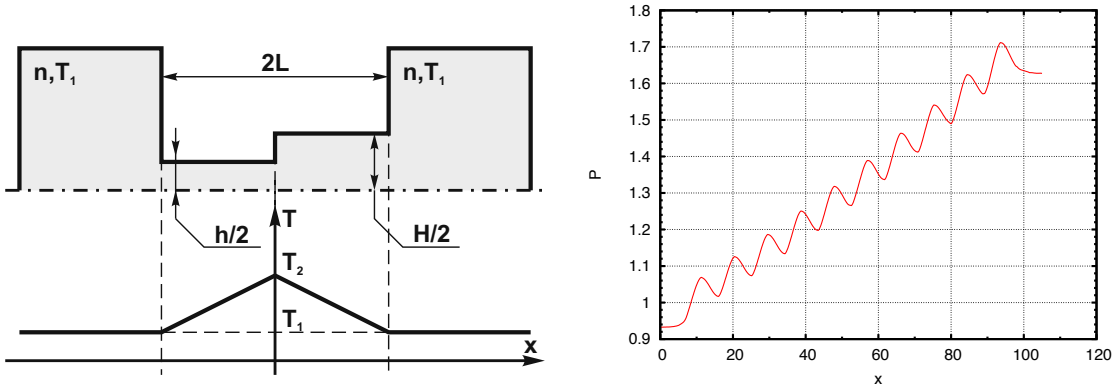

Figure 2: (a) Geometry of a simple multistage Knudsens pump and its wall temperature (b) Distribution of pressure along the channel axis of the 10-stage pump

Another pump design is shown in plane geometry in Figure 2(a). The pump consists of two channels of different width that produces a gas flow directed from the narrow channel to the wide one. It was precisely this design that was studied by Knudsen in 1910 [17].

The calculation was performed for the following values of dimensionless parameters: $T_1 = 1, T_2 = 2, H = 2h, L/h = 16/7$.

Figure 3 shows steady-state flow fields for two Knudsen numbers defined from the half-width of the narrow channel. Figure 2(b) shows steady-state distribution of pressure along the channel axis for a cascade of 10 pumping units at $\mathrm{Kn} = 0.5$ as shown in Figure 2(a).

3.2. Simulation of a 3D single-stage Knudsen pump

The device represents a long cylindrical tube consisting of a narrow channel with radius r and a wide channel of radius $R > r$. Along the wide channel, the temperature increases linearly from T_1 to $T_2 > T_1$, and along the narrow one the temperature decreases linearly from T_2 to T_1. An unstructured tetrahedral grid is built in the physical space as shown in Figure 4(a).

The grid was built with the GMSH code [18] using the Delaunay triangulation method optimized by means of the Netgen algorithm.

Let us describe the pumping process for argon at $r/\lambda = 1.25$, $T_2/T_1 = 1.5$. The pumping level will be characterized by the pressure ratio $a = p_2/p_1$, where p_1 is the gas pressure in the vessel being pumped out and p_2 the gas pressure in the vessel being pumped in. The value $t_0 = \sqrt{kT_0/(m\lambda^2)}$ is taken as time unit. Figure 5(a) shows the level of pumping versus time for the hard spheres potential and Lennard-Jones potential.

Figure 4(b) shows steady-state pressure distribution produced with the help of the Paraview code [19]. Figure 5(b) presents a plot of gas pumping versus Knudsen number. The most efficient mode of the pump operation is implemented at $\lambda = r$.

3.3. Gas mixture separation in a Knudsen pump

The possibility of separating a gas mixture in a Knudsen pump is studied in plane geometry. The system geometry is shown in Figure 8(a). There is considered a binary mixture of molecules representing hard spheres having the same diameter but different masses $m_1 = 10m$, $m_2 = m$, which corresponds to the

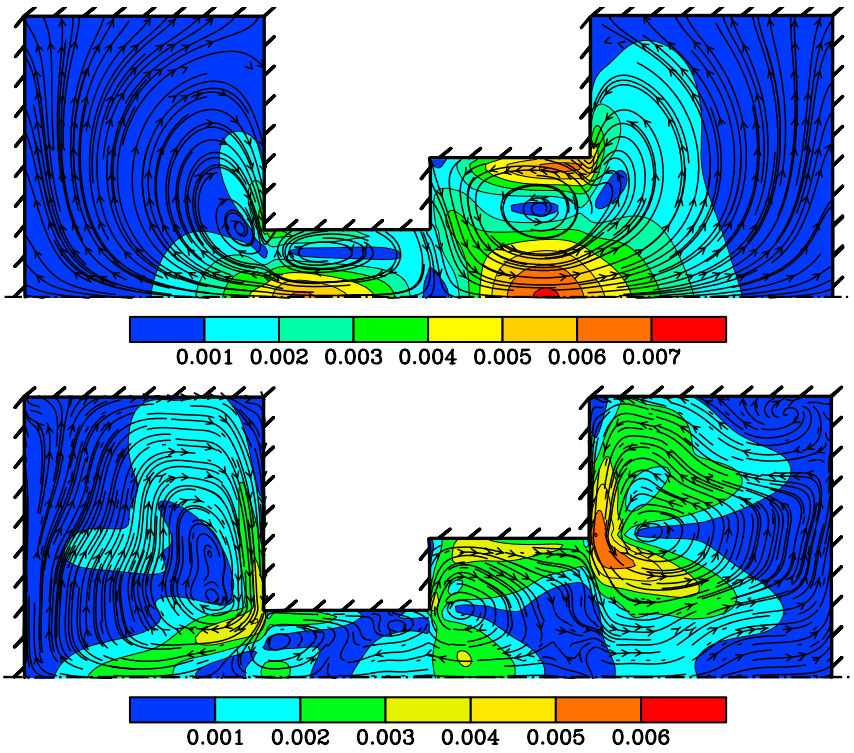

Figure 3: Steady-state flow distribution for different Knudsen numbers: (a) Kn = 0.1, (b) Kn = 1.5

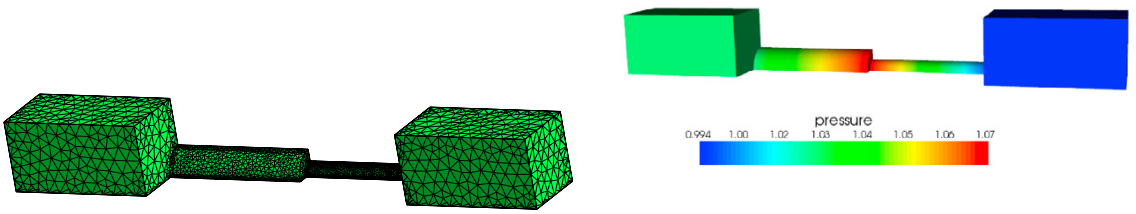

Figure 4: (a) Unstructured mesh for 3D Knudsen pump (b) Steady-state pressure distribution

helium-argon mixture. The initial ratio of gas concentrations was chosen as $n_1/n_2 = 2/1$ and the initial pressure in the system $p = const$. The wall temperature of the left-hand and right-hand vessels is maintained at $T_1 = T$ and $T_2 = 0.5T$, respectively and decreases linearly from T_1 to T_2 along the walls of the slit channel.

Main parameters under observation is the pumping $\Delta p(t)/p$ and concentrations of the mixture components in the left-hand and right-hand vessels $\eta_1(t) = n_1(t)/(n_1+n_2)$ and $\eta_2(t) = n_2(t)/(n_1+n_2)$. Respective curves are shown in Figures 6(a), 6(b), 6(c). The pressures and concentrations were measured in points A and B. It should be noted the pumping does not monotonically vary with time. This can be explained by

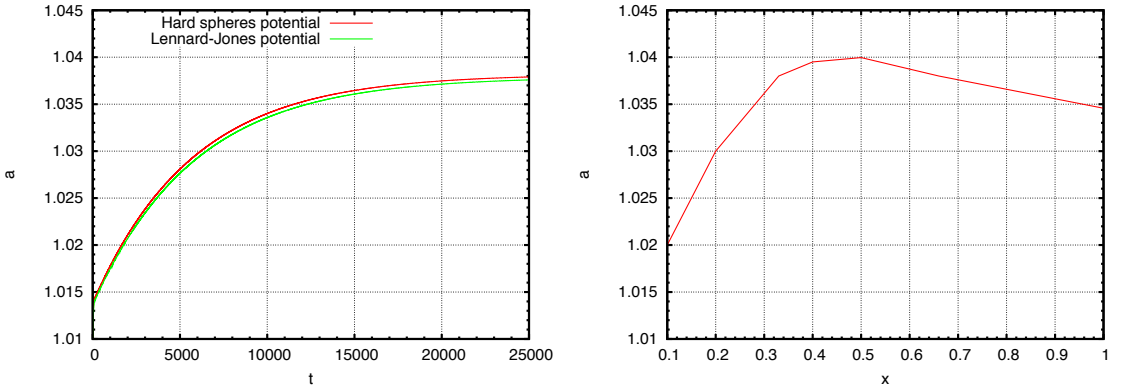

Figure 5: (a) Pumping versus time (b) Pumping versus Knudsen number

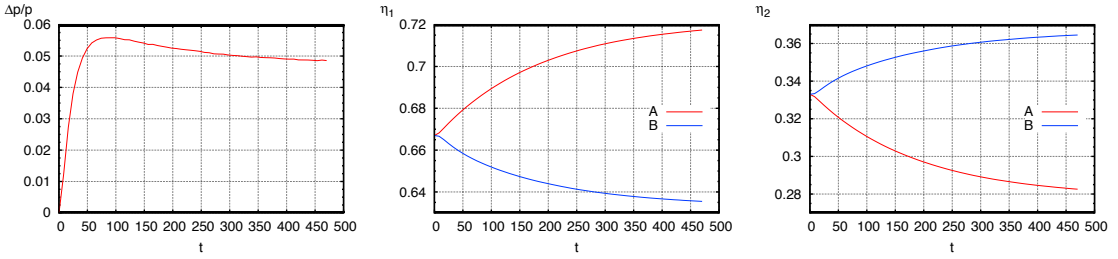

Figure 6: (a) pumping evolution (b) concentrations in the left-hand vessel (c) concentrations in the right-hand vessel

light molecules fairly quickly transferring to the left-hand vessel thus building up pressure in that vessel, with heavy molecules leaving the vessel at a much lower rate. The maximum pumping falls on the 15000-th time step, which corresponds to $\tau = 100$. At the 75000-th step the pumping attains a constant level of 4.8%. Figures 7(a), 7(b) show the pressure fields and concentration ratios fields at the 75000-th time step.

3.4. Shock wave incidence on a periodic slit structure

Incidence of a plane shock wave (SW) on a periodic structure consisting of microslits is considered. The problem geometry is shown in Figure 8(b), where CDE is the diffuse reflection slit wall. The length of segment CD is twice the width of slit h. The wall temperature is equal to the undisturbed gas temperature, AC and HF are symmetry lines with mirror boundary conditions. The boundary condition set on AH represents the Maxwellian function with parameters beyond the SW, that on EF – the Maxwellian function with undisturbed gas parameters and on BG – the initial position of the SW. The initial structure of the incident wave in the form of molecular velocity distribution function is calculated in advance on the basis of a one-dimensional SW problem and placed in the computational domain with the center on line BG.

The simulation was performed for the incident wave Mach number $M = 3$ and several Knudsen numbers $\mathrm{Kn} = 2\lambda/h$, where λ is the free path in the undisturbed gas and h is the slit width. Figures 9(a), 9(b) present results of calculations for the gas of hard spheres molecules at $\mathrm{Kn} = 0.05$ and times 9.6, 138.2, respectively. Values of main parameters of the gas along the slit center (density, temperature, longitudinal velocity component and local Mach number) are shown at the top of each figure. Early in the process, at $t = 9.6$, the gas velocity on the flow symmetry line behind the slit entrance is higher than the velocity beyond the entrance. The SW is slightly amplified. It is seen from the flow fields that at that moment the maximums of the velocity and temperature are at some distance from the symmetry line rather than in the

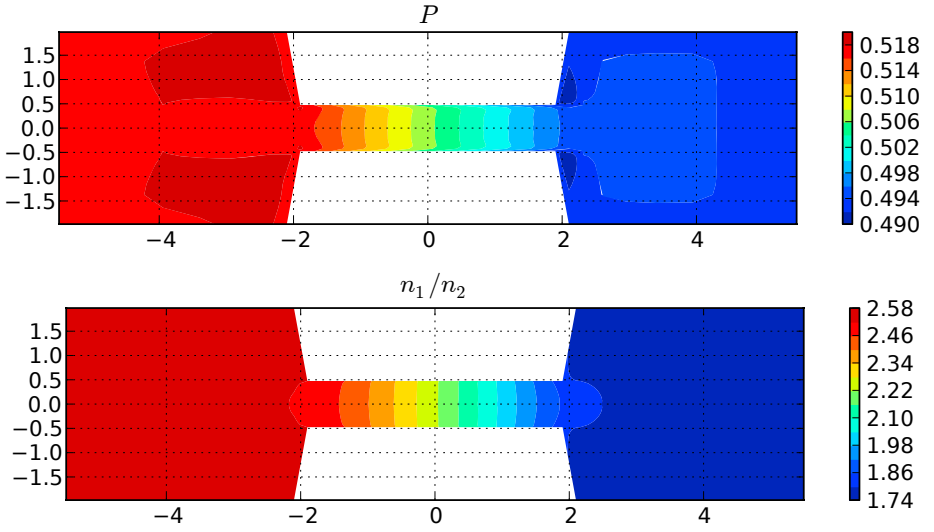

Figure 7: (a) Pressure field at the 75000-th step (b) Concentration ratio field at the 75000-th step

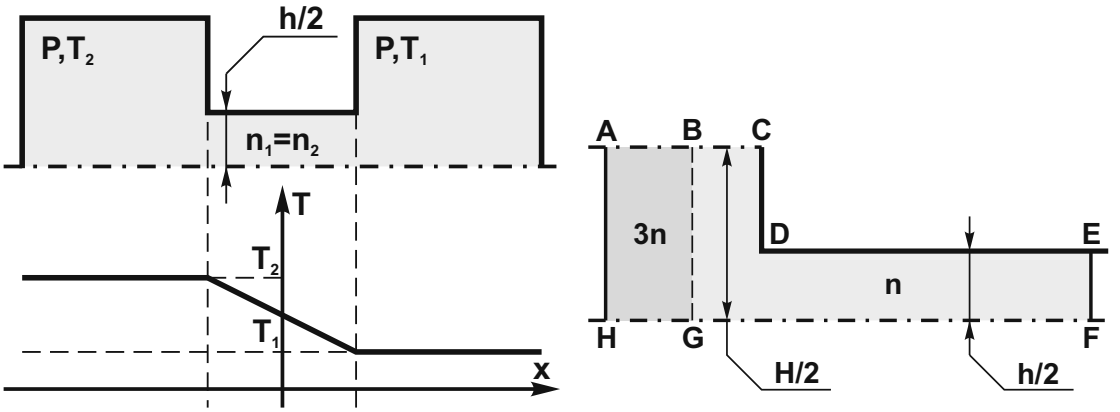

Figure 8: (a) Device geometry (b) Computational domain for shock wave problem

slit center. Near the symmetry line the SW structure is close to that of the plane SW. Subsequently the flow decelerates and the temperature and velocity maximums move to the central line. Reflected SW forming can be observed to the left of the slit entrance.

4. Conclusion

The examples above show that the developed methodology of solving the Boltzmann equation allows one to efficiently calculate flows of simple gases and gas mixtures in micro- and nanosize channels. It can be used both for calculation of slow slightly disturbed flows and for simulation of nonsteady supersonic flows with shock waves.

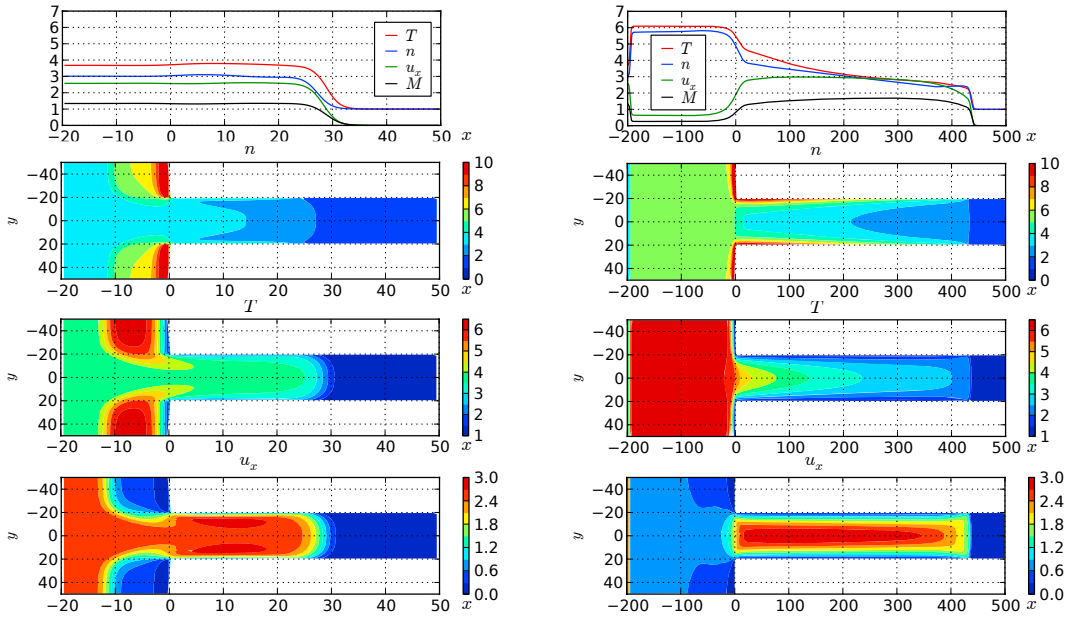

Figure 9: (a) Gas parameters for Kn = 0.05 at $t = 9.6$ (b) Gas parameters for Kn = 0.05 at $t = 138.2$

References

[1] S. E. Vargo, E. P. Muntz, An evaluation of a multiple stage micromechanical Knudsen compressor and vacuum pump, in: C. Shen (Ed.), Rarefied Gas Dynamics, Peking University Press, 1997, pp. 995–1000.

[2] Y. L. Han, A. Alexeenko, M. Young, P. E. Muntz, Experimental and computational studies of temperature gradient driven molecular transport in gas flows through nano/micro-scale channels, in: Second Intern. Conf. on Transport Phenomena in Micro and Nanodevices, Barga, Italy, 2006, pp. 583–601.

[3] G. A. Bird, Molecular Gas Dynamics and the Direct Simulation of Gas Flows, Clarendon Press, Oxford University Press, Oxford, 1994.

[4] J. M. Reese, M. A. Gallis, D. A. Lockerby, New directions in fluid dynamics: non-equilibrium aerodynamic and microsystem flows, Phil. Trans. R. Soc. Lond. A 361 (1813) (2003) 2967–2988.

[5] S. Chapman, T. G. Cowling, The Mathematical Theory of Nonuniform Gases, Cambridge Univ. Press, Cambridge, 1952.

[6] F. G. Tcheremissine, A conservative method for calculation of the Boltzmann collision integral, Doklady Physics 42 (11) (1997) 607–610.

[7] F. G. Tcheremissine, Solution of the Boltzmann kinetic equation for high-speed flows, Comp.Math. and Math.Physics 46 (2) (2006) 315–329.

[8] F. G. Tcheremissine, Solution of the Boltzmann kinetic equation for low speed flows, Transport Theory and Statistical Physics 37 (5) (2008) 564–575.

[9] N. M. Korobov, Trigonometric Sums and Their Applications, Moscow. Nauka, 1989, in russian.

[10] A. Raines, Study of a shock wave structure in gas mixtures on the basis of the Boltzmann equation, European Journal of Mechanics B/Fluids 21 (5) (2002) 599–610.

[11] F. G. Tcheremissine, R. K. Agarwal, A conservative numerical method for solving the generalized Boltzmann equation for an inert mixture of diatomic gases, in: AIAA Paper 2009-1581, Orlando, 2009.

[12] J. H. Ferziger, H. G. Kaper, Mathematical Theory of Transport Processes in Gases, North-Holland, Amsterdam, 1972.

[13] F. G. Cheremisin, Solution of the Wang Chang – Uhlenbeck master equation, Doklady Physics 47 (2002) 872–875.

[14] F. G. Tcheremissine, Two level kinetic model for rotational-translational transfers in a rarefied gas.
URL `http://www.chemphys.edu.ru/pdf/2007-10-22-001.pdf`

[15] Y. Y. Kloss, F. G. Tcheremissine, N. I. Khokhlov, B. A. Shurygin, Programming and modelling environment for studies of gas flows in micro- and nanostructures based on solving the Boltzmann equation, Atomic Energy 105 (4) (2008) 211–217.

[16] Y. Y. Kloss, F. G. Tcheremissine, N. I. Khokhlov, B. A. Shurygin, Development of numerical schemes for solving the kinetic equation in cluster environments based on MPI, Information processes 7 (4), in russian.
URL `http://www.jip.ru/2007/425-431-2007.pdf`

[17] M. Knudsen, Eine Revision der Gleichgewichtsbedingung der Gase. Thermische Molekularströmung, Ann. der Phys. 31 (9) (1910) 205–229.
[18] Gmsh homepage.
URL www.geuz.org/gmsh/
[19] Paraview homepage.
URL http://www.paraview.org/